

File SFPHYS1.DOC contains the following bookmarks. Select the topic you are trying to find from the list and double click the highlighted text.

[AnisotropicMagnetostatics](#)
[ElectromagneticTheory](#)
[MaxwellEquations](#)
[PermanentMagnetQuadWith16Wedges](#)
[VariableEasyAxisDirection](#)

Physics discussions in other files

SFPHYS2.DOC	Properties of static magnetic and electric fields
SFPHYS3.DOC	Boundary conditions and symmetries
SFPHYS4.DOC	Numerical methods in Poisson and Pandira
SFPHYS5.DOC	RF cavity theory

File SFPHYS1.DOC Table of Contents

XX. Theory of Electrostatics and Magnetostatics	531
A. Maxwell's equations	531
B. Isotropic magnetostatics in Cartesian coordinates	532
C. Isotropic electrostatics in Cartesian coordinates	534
D. Isotropic magnetostatics in cylindrical coordinates	536
E. Isotropic electrostatics in cylindrical coordinates	537
F. Anisotropic magnetostatics in Cartesian coordinates	539
1. Easy axis in a fixed direction	540
2. Easy axis on an off-center circle	543
G. Anisotropic electrostatics in Cartesian coordinates	545
H. Anisotropic magnetostatics in cylindrical coordinates	547
I. Anisotropic electrostatics in cylindrical coordinates	548

XX. Theory of Electrostatics and Magnetostatics

This section is based upon the chapter of the same title in Part B, Chapter 13.1 by John L. Warren in the 1987 publication Reference Manual for the POISSON/SUPERFISH Group of Codes, LA-UR-87-126. We reproduce it here in essentially its original form as reference material to the physics in the Poisson Superfish codes. The equation sequence numbers are the same as in the original. We have corrected a few typographical errors in the original, including the following:

- All occurrences of ∇V in Equations XX-113 and XX-114 should be $-\nabla V$.
- The D_{cY} and D_{cX} terms in Equation XX-115 should be negative.
- The correspondences in Equations XX-122 and XX-123 should have subscripts x and y interchanged on the left hand sides.

We have made a minor change in usage of the coercive force H_c . In the original version of Figure XX-5, which shows the B-H relation for an anisotropic material, the point on the horizontal axis was labeled “ $-H_c$ ” implying that H_c itself is a positive number. To be consistent with the input of the quantities BCEPT and HCEPT in Automesh, we omit the minus sign in Figure XX-5. Automesh expects the sign of HCEPT to be positive.

A. Maxwell's equations

We begin with Maxwell's Equations:

$$\nabla \times \mathbf{E} + \partial \mathbf{B} / \partial t = 0, \quad (\text{XX-1})$$

$$\nabla \times \mathbf{H} - \partial \mathbf{D} / \partial t = \mathbf{J}, \quad (\text{XX-2})$$

$$\nabla \cdot \mathbf{B} = 0, \quad (\text{XX-3})$$

$$\nabla \cdot \mathbf{D} = \rho. \quad (\text{XX-4})$$

Equations XX-2 and XX-4 imply the equation of continuity

$$\nabla \cdot \mathbf{J} + \partial \rho / \partial t = 0. \quad (\text{XX-5})$$

Maxwell's equations cannot be solved without assuming some relations among the vectors \mathbf{E} , \mathbf{B} , \mathbf{D} , \mathbf{H} , and \mathbf{J} . In vacuum the relations are

$$\mathbf{D} = \epsilon_0 \mathbf{E}, \quad (\text{XX-6})$$

$$\mathbf{H} = \mathbf{B} / \mu_0, \quad (\text{XX-7})$$

$$\mathbf{J} = \sum_{i=1}^N \mathbf{J}_i, \quad (\text{XX-8})$$

$$\rho = \sum_{i=1}^N \rho_i, \quad (\text{XX-9})$$

$$\text{where} \quad d\mathbf{J}_i/dt = \sum_{j \neq i} (e/m)_j [\rho_j \mathbf{E} + \mathbf{J}_j \times \mathbf{B}], \quad i = 1, \dots, N, \quad (\text{XX-10})$$

and where the summation is over all ionic species present. Equation XX-10 is the Lorentz force equation under the assumption that charge and mass are quantized and that relativistic and radiation damping effects can be ignored. This relation for \mathbf{J} is just illustrative of the type of equation needed to close the system but will not be used here.

Both Poisson and Pandira can solve problems involving isotropic solid material. Pandira also can handle anisotropic materials, which will be discussed later. In isotropic solids, which are the only materials Poisson can handle, one can write with adequate generality

$$\mathbf{D} = \varepsilon(\mathbf{x}, t, |\mathbf{E}|) \mathbf{E} = \kappa_e(\mathbf{x}, t, |\mathbf{E}|) \varepsilon_0 \mathbf{E}, \quad (\text{XX-11})$$

$$\mathbf{H} = \gamma(\mathbf{x}, t, |\mathbf{B}|) \mathbf{B} / \mu_0, \quad (\text{XX-12})$$

$$\mathbf{J} = \sigma(\mathbf{x}, t, |\mathbf{E}|) \mathbf{E}, \quad (\text{XX-13})$$

where the relative permittivity κ_e , the reluctivity γ , and the conductivity σ are usually piecewise constant functions of \mathbf{x} . Note that the reluctivity γ is the reciprocal of the relative permeability κ_m . For fields slowly varying in time, the time dependence of ε and γ can be ignored. The case of rapidly oscillating fields is discussed in the section on [rf cavity theory](#) for the code Superfish. Let us look at static problems first.

Poisson and Pandira solve a generalized integral form of Poisson's equation in two-dimensional, Cartesian coordinates or in cylindrically symmetric three-dimensional coordinates. This integral form of Poisson's equation works for both magnetostatics and electrostatics. It also handles both isotropic and anisotropic materials. In the following subsections we will start with the integral equation and show how it is related to Maxwell's and Poisson's equations.

B. Isotropic magnetostatics in Cartesian coordinates

The integral form of Equation XX-2 is

$$\oint_C \gamma(\mathbf{x}, |\mathbf{B}|) \nabla \times \mathbf{A} \cdot d\mathbf{l} = \mu_0 \int_V \mathbf{J} \cdot d\mathbf{a}, \quad (\text{XX-14})$$

where we have assumed that the displacement field \mathbf{D} has no time dependence. The contour C encloses the area A as shown in Figure XX-1. The magnetic induction \mathbf{B} is related to the vector potential \mathbf{A} by the equation

$$\mathbf{B} = \nabla \times \mathbf{A}. \quad (\text{XX-15})$$

One obtains the generalized Poisson equation by the following two steps:

$$\oint_C \gamma \nabla \times \mathbf{A} \cdot d\mathbf{l} = \int_A \nabla \times (\gamma \nabla \times \mathbf{A}) \cdot d\mathbf{a} = \int_A \mu_0 \mathbf{J} \cdot d\mathbf{a}, \quad (\text{XX-16})$$

$$\nabla \times (\gamma \nabla \times \mathbf{A}) = \mu_0 \mathbf{J}. \quad (\text{XX-17})$$

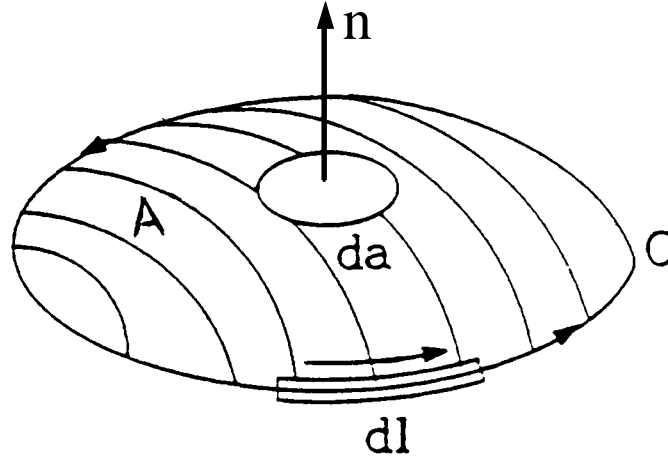


Figure XX-1. The geometry of the line and area integrals.

Equation XX-17 does not look like Poisson's equation, but in two-dimensional Cartesian coordinates, it reduces to Poisson's equation in the following way. Let us assume that \mathbf{A} is only a function of two coordinates (x, y) and that \mathbf{B} has only two nonzero components, B_x and B_y . Equation XX-15 requires that

$$B_x = \frac{\partial A_z}{\partial y} - \frac{\partial A_y}{\partial z} = \frac{\partial A_z}{\partial y}, \quad (\text{XX-18})$$

$$B_y = \frac{\partial A_x}{\partial z} - \frac{\partial A_z}{\partial x} = -\frac{\partial A_z}{\partial x}, \quad (\text{XX-19})$$

$$B_z = \frac{\partial A_y}{\partial x} - \frac{\partial A_x}{\partial y} = 0. \quad (\text{XX-20})$$

Equation XX-20 is satisfied if A_x and A_y are required to be identically zero. This requirement also satisfies the gauge relation

$$\nabla \cdot \mathbf{A} = \frac{\partial A_x}{\partial x} + \frac{\partial A_y}{\partial y} + \frac{\partial A_z}{\partial z} = 0. \quad (\text{XX-21})$$

It is easily seen that Equation XX-17 becomes

$$\frac{\partial}{\partial x} \left(\gamma \frac{\partial A_z}{\partial x} \right) + \frac{\partial}{\partial y} \left(\gamma \frac{\partial A_z}{\partial y} \right) = -\mu_0 \mathbf{J}_z, \quad (\text{XX-22})$$

$$\mathbf{J}_x = \mathbf{J}_y = 0. \quad (\text{XX-23})$$

The latter equation forces the current to be parallel to \mathbf{A} and Equation XX-22 is the generalized form of Poisson's equation. Equation XX-14 in two dimensions reduces to

$$\oint_C \gamma(\mathbf{x}, y, |\mathbf{B}|) \left[\frac{\partial A_z}{\partial y} dx - \frac{\partial A_z}{\partial x} dy \right] = \mu_0 \int_A \mathbf{J}_z dx dy. \quad (\text{XX-24})$$

For a small enough area A , we can assume that γ and \mathbf{J}_z are nearly constant and that A_z is a linear function of x and y , which we can write as

$$A_z \cong -b_x x + b_y y + a_0. \quad (\text{XX-25})$$

The integrals become

$$\left[\gamma(b_x, b_y) \oint_C dx \right] b_x + \left[\gamma(b_x, b_y) \oint_C dy \right] b_y = \mu_0 \mathbf{J}_z A. \quad (\text{XX-26})$$

This is a nonlinear equation with two unknowns, b_x and b_y . It is the sort of equation that is created at each mesh point in the Poisson solver code. [Chapter XXI](#) explains how the set of mesh-point equations are solved to obtain numerically the vector potential A_z .

C. Isotropic electrostatics in Cartesian coordinates

The integral form of Equation XX-4 is

$$\oint_S \kappa_e(\mathbf{x}, |\mathbf{E}|) \nabla V(\mathbf{x}) \cdot d\mathbf{s} = -\frac{1}{\epsilon_0} \int_V \rho(\mathbf{x}) dv, \quad (\text{XX-27})$$

where $V(\mathbf{x})$ is the scalar potential and the integral on the right is over a volume V whose surface is denoted by S . The electric field is \mathbf{E} given by

$$\mathbf{E} = -\nabla V. \quad (\text{XX-28})$$

It is well known that Equation XX-27 is equivalent to the differential equation

$$\nabla \cdot (\kappa_e \nabla V) = -\rho / \epsilon_0. \quad (\text{XX-29})$$

In two-dimensional Cartesian coordinates this equation becomes

$$\frac{\partial}{\partial x}(\kappa_e V) + \frac{\partial}{\partial y}(\kappa_e V) = -\rho/\epsilon_0. \quad (\text{XX-30})$$

The similarity to Equation XX-22 is obvious. The integral form of the equation can also be made to resemble Equation XX-24 as follows. Suppose that κ_e , $V(\mathbf{x})$, and $\rho(\mathbf{x})$ are functions only of (x, y) . Take the volume V to be a generalized cylinder of cross section A and length L as shown in Figure XX-2. Since $V(\mathbf{x})$ is only a function of (x, y) , ∇V has only x and y components. This statement says that the surface integral over the flat ends of the volume cannot contribute to the integral because the direction of the normal vectors for these areas is perpendicular to ∇V . The integral over the area of the cylindrical surface can be written as

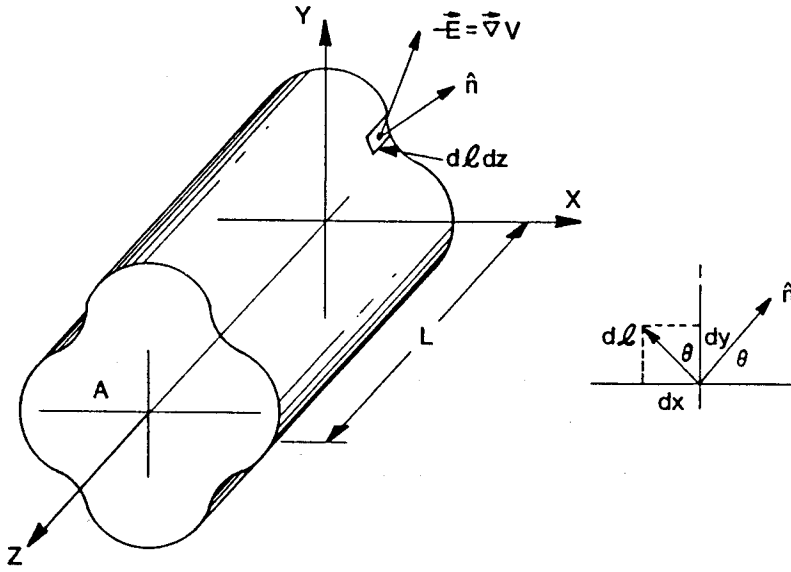


Figure XX-2. Cylindrical volume in Cartesian coordinates.

The volume V has a uniform cross section of area A and length L . The inset shows the relation between the normal vector angle \hat{n} and element of length dl .

$$\oint_S \kappa_e \nabla V \cdot d\mathbf{s} = \oint_C \int_0^L \kappa_e \nabla V \cdot \hat{n} dz dl, \quad (\text{XX-31})$$

where \hat{n} is the outward normal vector to the surface and dl is an element of length on the contour C . The integral over z evaluates to L and the quantity $\hat{n} dl$ can be written in Cartesian coordinates as

$$\hat{n} dl = dl \cos \theta \hat{e}_x + dl \sin \theta \hat{e}_y. \quad (\text{XX-32})$$

From Figure XX-2 we see that

$$dx = -dl \sin \theta, \quad (\text{XX-33})$$

$$dy = dl \cos \theta, \quad (\text{XX-34})$$

$$\text{and hence} \quad \hat{\mathbf{n}} d\mathbf{l} = dy \hat{\mathbf{e}}_x - dx \hat{\mathbf{e}}_y. \quad (\text{XX-35})$$

When this relation is put into Equation XX-31, the result is

$$\oint_S \kappa_e \nabla V \cdot d\mathbf{s} = -L \oint_C \kappa_e \left[\frac{\partial V}{\partial y} dx - \frac{\partial V}{\partial x} dy \right]. \quad (\text{XX-36})$$

The integral over the volume V can be written as

$$\frac{1}{\epsilon_0} \int_V \rho dV = \frac{L}{\epsilon_0} \int_A \rho dx dy. \quad (\text{XX-37})$$

This means that Equation XX-27 can be written as

$$\oint_C \kappa_e(x, y, |\mathbf{E}|) \left[\frac{\partial V}{\partial y} dx - \frac{\partial V}{\partial x} dy \right] = \frac{1}{\epsilon_0} \int_A \rho dx dy. \quad (\text{XX-38})$$

Comparison with Equation XX-24 makes it clear that there is a correspondence between the following pairs of quantities

$$V \rightarrow A_z, \quad (\text{XX-39})$$

$$\kappa_e \rightarrow \gamma, \quad (\text{XX-40})$$

$$\frac{1}{\epsilon_0} \rightarrow \mu_0, \quad (\text{XX-41})$$

$$\rho \rightarrow J_z, \quad (\text{XX-42})$$

The same correspondences come out of a comparison between Equations XX-22 and XX-30.

D. Isotropic magnetostatics in cylindrical coordinates

We assume that \mathbf{A} is only a function of (r, z) and not the cylindrical angle θ . The expressions for the components of \mathbf{B} are

$$B_r = (\nabla \times \mathbf{A})_r = \frac{1}{r} \frac{\partial A_z}{\partial \theta} - \frac{\partial A_\theta}{\partial z} = -\frac{\partial A_\theta}{\partial z}, \quad (\text{XX-43})$$

$$B_z = \frac{1}{r} \frac{\partial}{\partial r} (r A_\theta) - \frac{1}{r} \frac{\partial A_r}{\partial \theta} = \frac{1}{r} \frac{\partial}{\partial r} (r A_\theta), \quad (\text{XX-44})$$

$$B_\theta = \frac{\partial A_r}{\partial z} - \frac{\partial A_z}{\partial r} = 0. \quad (\text{XX-45})$$

Here we have assumed that \mathbf{B} lies in the r - z plane. We choose the condition that

$$A_r = A_z = 0, \quad (\text{XX-46})$$

which automatically satisfies the gauge condition $\nabla \cdot \mathbf{A} = 0$. Equation XX-14 written in cylindrical coordinates is

$$\oint_C \frac{\gamma}{r} \left[\frac{\partial}{\partial z} (r A_\theta) dr - \frac{\partial}{\partial r} (r A_\theta) dz \right] = \mu_0 \int_A J_\theta dr dz, \quad (\text{XX-47})$$

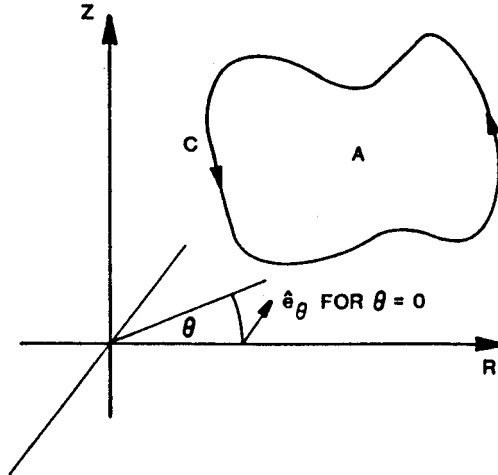


Figure XX-3. Area and contour path in cylindrical coordinates.

If the contour is taken in the counterclockwise direction, then the area has a normal vector in the $-\hat{e}_\theta$ direction. This fact is important in deriving Equation XX-47.

where we have introduced a factor of r into the derivative with respect to z for symmetry. Figure XX-3 shows the geometry. There is a correspondence used in the codes between quantities in cylindrical and Cartesian coordinates given by the relations

$$r \rightarrow x, \quad (\text{XX-48})$$

$$z \rightarrow y, \quad (\text{XX-49})$$

$$r A_\theta \rightarrow -A_z, \quad (\text{XX-50})$$

$$J_\theta \rightarrow -J_z, \quad (\text{XX-51})$$

$$\frac{\gamma}{r} \rightarrow \gamma. \quad (\text{XX-52})$$

E. Isotropic electrostatics in cylindrical coordinates

We assume that the scalar potential is only a function of (r, z) . The electric field has only r and z components, which are given by

$$E_r = -\frac{\partial V}{\partial r}, \quad (\text{XX-53})$$

$$E_z = -\frac{\partial V}{\partial z}. \quad (\text{XX-54})$$

The volume of integration in Equation XX-27 is a torus of cross sectional area A as illustrated in Figure XX-4. Integration over the angle θ evaluates to 2π and Equation XX-27 can be expressed as

$$2\pi \oint_C \kappa_e \nabla V \cdot \hat{n} r dl = -\frac{2\pi}{\epsilon_0} \int_A \rho r dr dz. \quad (\text{XX-55})$$

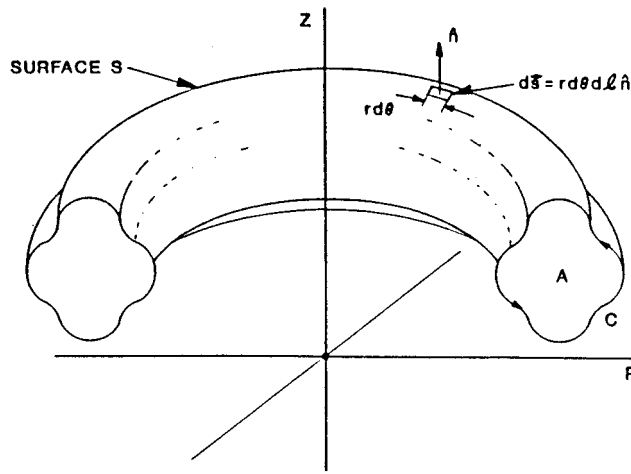


Figure XX-4. Volume in cylindrical coordinates.

The figure shows the geometry of the volume V , surface S , cross sectional area A , and contour C . The normal vector \hat{n} to the area A is in the $-\hat{e}_\theta$ direction.

By analogy to Equation XX-35, one can show that

$$\hat{n} dl = dz \hat{e}_r - dr \hat{e}_z, \quad (\text{XX-56})$$

and hence Equation XX-55 becomes

$$\oint_C \kappa_e r \left[\frac{\partial V}{\partial z} dr - \frac{\partial V}{\partial r} dz \right] = \frac{1}{\epsilon_0} \int_A \rho r dr dz. \quad (\text{XX-57})$$

Comparison with the magnetostatic equation in Cartesian coordinates, Equation XX-24, gives the following correspondences

$$r \rightarrow x, \quad (\text{XX-58})$$

$$z \rightarrow y, \quad (\text{XX-59})$$

$$V \rightarrow A_z, \quad (\text{XX-60})$$

$$\kappa_e \mathbf{r} \rightarrow \gamma, \quad (\text{XX-61})$$

$$\frac{1}{\varepsilon_0} \rightarrow \mu_0. \quad (\text{XX-62})$$

$$r\rho \rightarrow \mathbf{J}_z. \quad (\text{XX-63})$$

Comparison with Equations XX-48 through XX-52 shows that $A_\theta(r, z)$ is not analogous to $V(r, z)$ in cylindrical coordinates.

F. Anisotropic magnetostatics in Cartesian coordinates

Historically, there was an attempt to modify Poisson to handle two-dimensional anisotropic materials, but the code's convergence was extremely poor. Halbach and Holsinger decided to write a new program called Pandira, which uses the so-called direct method rather than the successive over-relaxation method for the numerical solution of Maxwell's equations. Maxwell's equations become

$$\nabla \times \mathbf{H} = \mathbf{J}, \quad (\text{XX-64})$$

$$\nabla \cdot \mathbf{B} = 0, \quad (\text{XX-65})$$

$$\mathbf{B} = \nabla \times \mathbf{A}, \quad (\text{XX-66})$$

$$\mathbf{H} = \vec{\gamma} \cdot \mathbf{B} / \mu_0 + \mathbf{H}_c, \quad (\text{XX-67})$$

where $\vec{\gamma}$ is the reluctivity tensor and \mathbf{H}_c is the magnetic field when $\mathbf{B} = 0$, that is, the permanent magnetic field. Pandira handles anisotropic materials having an “easy axis” and a “hard axis” perpendicular to the easy axis,

$$\mathbf{H} = \mathbf{H}_\parallel + \mathbf{H}_\perp, \quad (\text{XX-68})$$

$$\mathbf{H}_\parallel = \gamma_\parallel \mathbf{B}_\parallel / \mu_0 + \mathbf{H}_c, \quad (\text{XX-69})$$

$$\mathbf{H}_\perp = \gamma_\perp \mathbf{B}_\perp / \mu_0, \quad (\text{XX-70})$$

or one can write the inverse relations

$$\mathbf{B}_\parallel = \kappa_{m\parallel} \mu_0 \mathbf{H}_\parallel + \mathbf{B}_r, \quad (\text{XX-71})$$

$$\mathbf{B}_\perp = \kappa_{m\perp} \mu_0 \mathbf{H}_\perp, \quad (\text{XX-72})$$

where $\gamma_\parallel = 1/\kappa_{m\parallel}, \quad (\text{XX-73})$

$$\gamma_\perp = 1/\kappa_{m\perp}, \quad (\text{XX-74})$$

$$\mathbf{B}_r = -\kappa_{m\parallel} \mu_0 \mathbf{H}_c, \quad (\text{XX-75})$$

and where \mathbf{B}_{\parallel} is parallel to the easy axis and \mathbf{B}_{\perp} is along the hard axis. The permeability relations are different in the two special directions. Figure XX-5 shows typical relations. The easy axis is characterized by the coercive force H_c and the remanent field B_r . Program Pandira allows two geometries for the easy axis. In the first geometry the easy axis is independent of position in the material. In the second geometry, the direction of the easy axis changes along the circumference of a circle that is not necessarily concentric with the origin of coordinates. These two geometries are explained below.

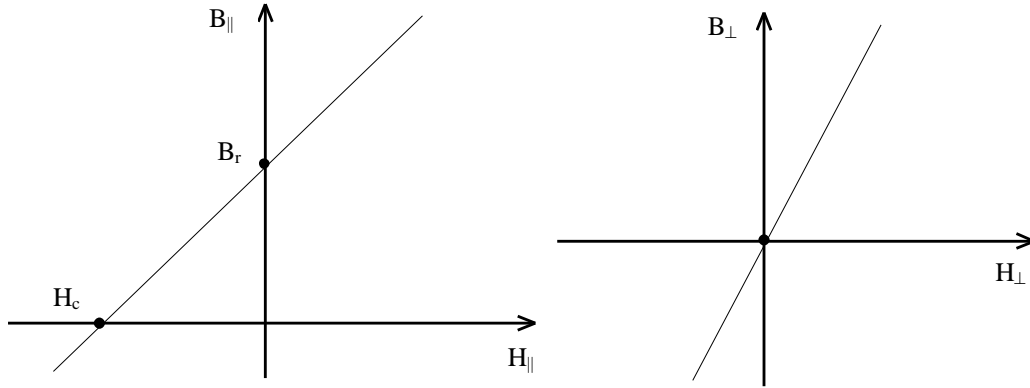


Figure XX-5. B-H relationships for an anisotropic material.

The left figure shows the coercive force H_c (in Oersteds) and the remanent field B_r (in Gauss) for fields parallel to the easy axis. For a non-permanent (but anisotropic) magnetic material, the curve goes through the origin like it does for the direction perpendicular to the easy axis shown at right.

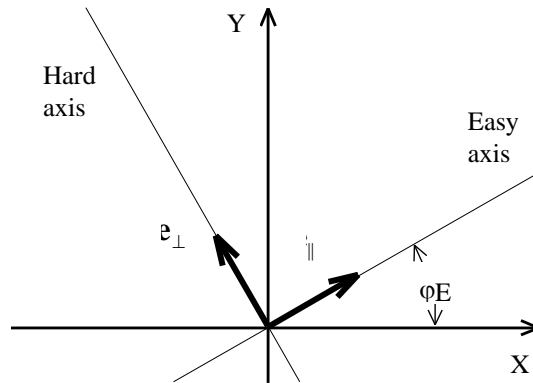


Figure XX-6. Unit vectors for anisotropic materials.

This figure defines the angle ϕ_E and the two unit vectors \hat{e}_{\parallel} and \hat{e}_{\perp} that lie along the easy and hard axes.

1. Easy axis in a fixed direction

Figure XX-6 shows the directions of the easy and hard axes relative to the coordinate axes in the region of interest. The field \mathbf{B} can be expressed in terms of the unit vectors for the two coordinate systems as

$$\mathbf{B} = B_X \hat{\mathbf{e}}_X + B_Y \hat{\mathbf{e}}_Y = B_{\parallel} \hat{\mathbf{e}}_{\parallel} + B_{\perp} \hat{\mathbf{e}}_{\perp}. \quad (\text{XX-76})$$

The unit vectors are related by the matrix transformation

$$\begin{pmatrix} \hat{\mathbf{e}}_{\parallel} \\ \hat{\mathbf{e}}_{\perp} \end{pmatrix} = \begin{pmatrix} \cos \varphi_E & \sin \varphi_E \\ -\sin \varphi_E & \cos \varphi_E \end{pmatrix} \begin{pmatrix} \hat{\mathbf{e}}_X \\ \hat{\mathbf{e}}_Y \end{pmatrix}. \quad (\text{XX-77})$$

The field \mathbf{H} takes the form

$$\mathbf{H} = \left(\gamma_{\parallel} B_{\parallel} / \mu_0 + H_c \right) \hat{\mathbf{e}}_{\parallel} + \left(\gamma_{\perp} B_{\perp} / \mu_0 \right) \hat{\mathbf{e}}_{\perp} = H_{\parallel} \hat{\mathbf{e}}_{\parallel} + H_{\perp} \hat{\mathbf{e}}_{\perp}, \quad (\text{XX-78})$$

from which one can deduce that

$$\mathbf{H} = \left(H_{\parallel} \cos \varphi_E + H_{\perp} \sin \varphi_E \right) \hat{\mathbf{e}}_X + \left(H_{\parallel} \sin \varphi_E - H_{\perp} \cos \varphi_E \right) \hat{\mathbf{e}}_Y. \quad (\text{XX-79})$$

By using the inverse transformation on the unit vectors, namely,

$$\begin{pmatrix} \hat{\mathbf{e}}_X \\ \hat{\mathbf{e}}_Y \end{pmatrix} = \begin{pmatrix} \cos \varphi_E & -\sin \varphi_E \\ \sin \varphi_E & \cos \varphi_E \end{pmatrix} \begin{pmatrix} \hat{\mathbf{e}}_{\parallel} \\ \hat{\mathbf{e}}_{\perp} \end{pmatrix}, \quad (\text{XX-80})$$

one can show that

$$\mathbf{B} = \left(B_X \cos \varphi_E + B_Y \sin \varphi_E \right) \hat{\mathbf{e}}_{\parallel} + \left(-B_X \sin \varphi_E + B_Y \cos \varphi_E \right) \hat{\mathbf{e}}_{\perp}. \quad (\text{XX-81})$$

This gives B_{\parallel} and B_{\perp} (and hence H_{\parallel} and H_{\perp}) in terms of B_X and B_Y . After making substitutions and solving for H_X and H_Y one obtains

$$H_X = \left(\gamma_{\parallel} \cos^2 \varphi_E + \gamma_{\perp} \sin^2 \varphi_E \right) \frac{B_X}{\mu_0} + \sin 2\varphi_E \left(\gamma_{\parallel} - \gamma_{\perp} \right) \frac{B_Y}{2\mu_0} - H_c \cos \varphi_E, \quad (\text{XX-82})$$

$$H_Y = \sin 2\varphi_E \left(\gamma_{\parallel} - \gamma_{\perp} \right) \frac{B_X}{2\mu_0} + \left(\gamma_{\parallel} \sin^2 \varphi_E + \gamma_{\perp} \cos^2 \varphi_E \right) \frac{B_Y}{\mu_0} - H_c \sin \varphi_E. \quad (\text{XX-83})$$

These equations can be written in matrix form as

$$\begin{pmatrix} H_X \\ H_Y \end{pmatrix} = \frac{1}{\mu_0} \begin{pmatrix} \gamma_{XX} & \gamma_{XY} \\ \gamma_{YX} & \gamma_{YY} \end{pmatrix} \begin{pmatrix} B_X \\ B_Y \end{pmatrix} - \begin{pmatrix} H_{cX} \\ H_{cY} \end{pmatrix}, \quad (\text{XX-84})$$

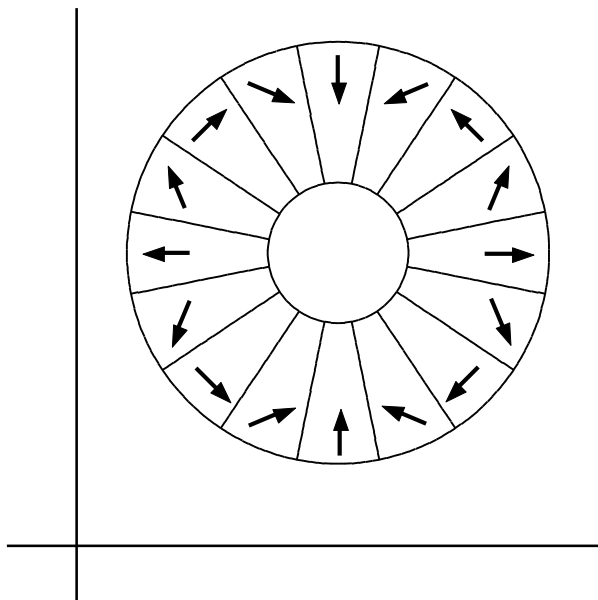


Figure XX-7. Permanent-magnet quadrupole.

This example, which is in the [LANL/Examples/Magnetostatic/PMQuads](#) directory, is a magnet constructed from wedge-shaped blocks of permanent magnet material with the easy axis in each block having a different orientation.

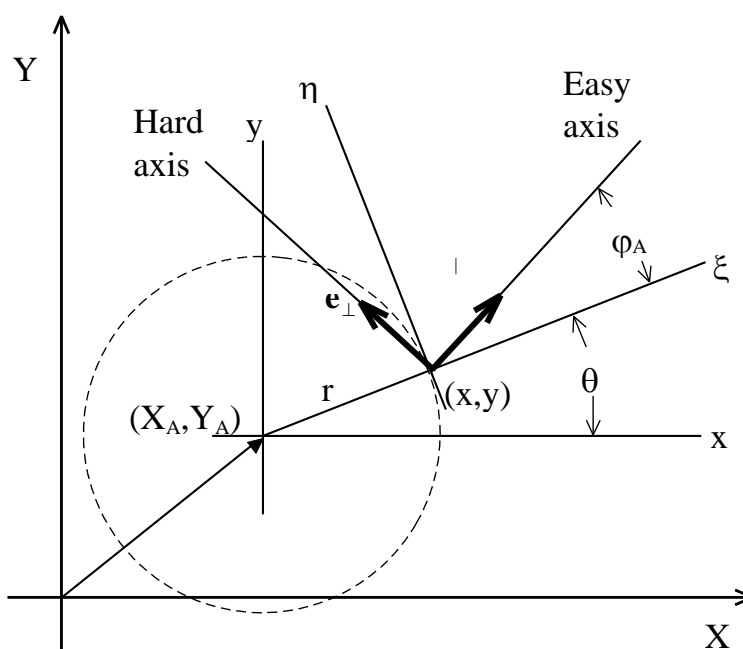


Figure XX-8. Definitions of parameters in off-center anisotropic materials.

where the following equations define the symmetric reluctivity tensor $\tilde{\gamma}$ and the components of the coercive force \mathbf{H}_c :

$$\gamma_{XX} = \gamma_{\parallel} \cos^2 \varphi_E + \gamma_{\perp} \sin^2 \varphi_E, \quad (\text{XX-85})$$

$$\gamma_{XY} = \frac{1}{2} \sin 2\varphi_E (\gamma_{\parallel} - \gamma_{\perp}), \quad (\text{XX-86})$$

$$\gamma_{YY} = \gamma_{\parallel} \sin^2 \varphi_E + \gamma_{\perp} \cos^2 \varphi_E, \quad (\text{XX-87})$$

$$H_{cX} = H_c \cos \varphi_E, \quad (\text{XX-88})$$

$$H_{cY} = H_c \sin \varphi_E. \quad (\text{XX-89})$$

2. Easy axis on an off-center circle

Pandira includes an option that allows the easy axis direction to be a function of angle around the center of a circle. Although there is no natural material for which the direction of the easy axis is a function of position in the plane, one can construct a magnet from blocks of permanent magnet material with each block having its own orientation as shown in Figure XX-7. One can think of the wedge magnet as approximating the idealized material. The chapter on [Automesh](#) describes how to use this option in an input file. The directory [LANL\Examples\Magnetostatic\PMQuads](#) includes a sample input file for a 16-wedge quadrupole magnet like the one in Figure XX-7. For comparison, this directory also has an example of the idealized case of continuously varying easy axis direction. We believe that variable-easy-axis option was added to Pandira because early versions of the code did not allow enough material types to solve the real problem. We recommend setting up the actual geometry for design work. The idealized option in Pandira may still be useful for visualizing a concept.

The center of the circle need not coincide with the origin of coordinates. Figure XX-8 shows the geometry of the easy axis in such a material. The origin of the easy axis is determined by the three parameters X_A , Y_A , and φ_A . Relating these parameters to reluctivity tensor $\tilde{\gamma}$ and the coercive force \mathbf{H}_c is a matter of coordinate transformations. There are three coordinate systems that enter into the formulation,

$$(\hat{\mathbf{e}}_{\parallel}, \hat{\mathbf{e}}_{\perp}) \rightarrow (\hat{\mathbf{e}}_{\xi}, \hat{\mathbf{e}}_{\eta}) \rightarrow (\hat{\mathbf{e}}_X, \hat{\mathbf{e}}_Y). \quad (\text{XX-90})$$

In the $(\hat{\mathbf{e}}_{\xi}, \hat{\mathbf{e}}_{\eta})$ system, the tensor $\tilde{\gamma}$ and the vector \mathbf{H}_c are the same as described in Equations XX-85 through XX-89 above. The axes $(\hat{\mathbf{e}}_{\xi}, \hat{\mathbf{e}}_{\eta})$ change as a function of (x, y) . The (x, y) coordinates are related to the (X, Y) coordinates by a linear transformation. Let

$$\mathbf{X} = X\hat{\mathbf{e}}_X + Y\hat{\mathbf{e}}_Y = (X_A + x)\hat{\mathbf{e}}_X + (Y_A + y)\hat{\mathbf{e}}_Y, \quad (\text{XX-91})$$

$$\text{and} \quad \begin{pmatrix} \hat{\mathbf{e}}_\xi \\ \hat{\mathbf{e}}_\eta \end{pmatrix} = \begin{pmatrix} \cos\theta & \sin\theta \\ -\sin\theta & \cos\theta \end{pmatrix} \begin{pmatrix} \hat{\mathbf{e}}_x \\ \hat{\mathbf{e}}_y \end{pmatrix}, \quad (\text{XX-92})$$

$$\text{where} \quad \cos\theta = \frac{X - X_A}{\sqrt{(X - X_A)^2 + (Y - Y_A)^2}}, \quad (\text{XX-93})$$

$$\text{and} \quad \sin\theta = \frac{Y - Y_A}{\sqrt{(X - X_A)^2 + (Y - Y_A)^2}}. \quad (\text{XX-94})$$

From Figure XX-8 one sees that

$$\begin{pmatrix} \hat{\mathbf{e}}_\parallel \\ \hat{\mathbf{e}}_\perp \end{pmatrix} = \begin{pmatrix} \cos\varphi_A & \sin\varphi_A \\ -\sin\varphi_A & \cos\varphi_A \end{pmatrix} \begin{pmatrix} \hat{\mathbf{e}}_x \\ \hat{\mathbf{e}}_y \end{pmatrix}. \quad (\text{XX-95})$$

Either by multiplication of the matrices or by looking at Figure XX-8 again, one can show that

$$\begin{pmatrix} \hat{\mathbf{e}}_\parallel \\ \hat{\mathbf{e}}_\perp \end{pmatrix} = \begin{pmatrix} \cos(\varphi_A + \theta) & \sin(\varphi_A + \theta) \\ -\sin(\varphi_A + \theta) & \cos(\varphi_A + \theta) \end{pmatrix} \begin{pmatrix} \hat{\mathbf{e}}_x \\ \hat{\mathbf{e}}_y \end{pmatrix}. \quad (\text{XX-96})$$

The derivation of the components of $\vec{\gamma}$ can be completed as we did before for the fixed direction case. The only difference is that φ_E is replaced by $\varphi_A + \theta(X, Y)$. The reluctivity tensor $\vec{\gamma}$ and the coercive force \mathbf{H}_c are now functions of the position in the material. In an MT namelist in the Automesh input file, the parameters are defined as follows:

$$\text{AEASY} = \varphi_E, \text{GAMPER} = \gamma_\perp, \text{HCEPT} = H_c, \quad (\text{XX-97})$$

and γ_\parallel is determined from B_r , that is, from Figure XX-5, where we see that

$$\gamma_\parallel = B_r / (\mu_0 H_c). \quad (\text{XX-98})$$

With this information as a background, we now write down the integral equation used in Pandira to find the vector potential, namely,

$$\oint_C [\vec{\gamma} \cdot \nabla \times \mathbf{A} + \mu_0 \mathbf{H}_c] \cdot d\mathbf{l} = \mu_0 \int_A \mathbf{J} \cdot d\mathbf{a}. \quad (\text{XX-99})$$

In Cartesian coordinates we once more choose the gauge

$$\nabla \cdot \mathbf{A} = 0, \quad (\text{XX-100})$$

which requires that

$$\mathbf{A} = A_z \hat{\mathbf{e}}_z, \quad (\text{XX-101})$$

$$\text{and} \quad \mathbf{J}_x = \mathbf{J}_y = 0. \quad (\text{XX-102})$$

Equation XX-24 becomes

$$\oint_C \left[\gamma_{xx} \frac{\partial A_z}{\partial y} - \gamma_{xy} \frac{\partial A_z}{\partial x} + \mu_0 H_{cx} \right] dx + \left[\gamma_{xy} \frac{\partial A_z}{\partial y} - \gamma_{yy} \frac{\partial A_z}{\partial x} + \mu_0 H_{cy} \right] dy = \mu_0 \int_A J_z dx dy. \quad (\text{XX-103})$$

This complication does not prevent one from applying the same numerical method discussed in [Chapter XXI](#) to find the solution. If A_z is a linear function of x and y as in Equation XX-25, then Equation XX-103 reduces to

$$\left[\gamma_{xx} \int_C dx + \gamma_{xy} \int_C dy \right] b_x + \left[\gamma_{xy} \int_C dx + \gamma_{yy} \int_C dy \right] b_y = \mu_0 \left[J_z A - H_{cx} \oint_C dx - H_{cy} \oint_C dy \right]. \quad (\text{XX-104})$$

This equation, like Equation XX-26, is still nonlinear in b_x and b_y . Since the γ 's are functions of b_x and b_y , the equation must be solved iteratively.

G. Anisotropic electrostatics in Cartesian coordinates

The basic equations for dielectric materials are

$$\nabla \cdot \mathbf{D} = \rho. \quad (\text{XX-105})$$

$$\nabla \times \mathbf{E} = 0, \quad (\text{XX-106})$$

$$\mathbf{E} = -\nabla V, \quad (\text{XX-107})$$

$$\mathbf{D} = \epsilon_0 \tilde{\mathbf{\kappa}}_e \cdot \mathbf{E} + \mathbf{D}_c, \quad (\text{XX-108})$$

As in the magnetostatic case, one can define an easy axis and a hard axis for the material. This definition results in relations analogous to Equations XX-68 through XX-89 with the correspondences

$$\mathbf{H} \rightarrow \mathbf{D}, \quad (\text{XX-109})$$

$$\mathbf{B} \rightarrow \mathbf{E}, \quad (\text{XX-110})$$

$$\gamma \rightarrow \kappa_e, \quad (\text{XX-111})$$

$$\mu_0 \rightarrow 1/\epsilon_0. \quad (\text{XX-112})$$

The coordinate transformations expressed in Equations XX-90 through XX-96 are the same. The integral equation for the scalar potential is a generalization of Equation XX-27, which was derived with the assumptions that $\kappa_e = 1$ and $\mathbf{D}_c = 0$. Divide equation XX-108 by ϵ_0 and substitute for \mathbf{E} from equation XX-107 to see that $\kappa_e(-\nabla V)$ can be replaced by the quantity $\kappa_e(-\nabla V) + \mathbf{D}_c/\epsilon_0$, resulting in the equation

$$\oint_S [\vec{\kappa}_e \cdot (-\nabla V) + \mathbf{D}_c/\epsilon_0] \cdot d\mathbf{s} = \frac{1}{\epsilon_0} \int_V \rho dv. \quad (\text{XX-113})$$

The derivation leading to Equation XX-36 is essentially unchanged. The final result is

$$\oint_S [\vec{\kappa}_e \cdot (-\nabla V) + \mathbf{D}_c/\epsilon_0] \cdot d\mathbf{s} = -L \left\{ \oint_C [\vec{\kappa}_e \cdot (-\nabla V) + \mathbf{D}_c/\epsilon_0]_y dx - \oint_C [\vec{\kappa}_e \cdot (-\nabla V) + \mathbf{D}_c/\epsilon_0]_x dy \right\}. \quad (\text{XX-114})$$

Again, the integral over z in the volume integral on the right-hand side of Equation XX-113 evaluates to L , so Equation XX-113 can be written in the form

$$\oint_C \left[\kappa_{eYX} \frac{\partial V}{\partial x} + \kappa_{eYY} \frac{\partial V}{\partial y} - \frac{D_{cY}}{\epsilon_0} \right] dx - \oint_C \left[\kappa_{eXX} \frac{\partial V}{\partial x} + \kappa_{eXY} \frac{\partial V}{\partial y} - \frac{D_{cX}}{\epsilon_0} \right] dy = \frac{1}{\epsilon_0} \int_A \rho dx dy. \quad (\text{XX-115})$$

A comparison with the magnetostatic result, Equation XX-103, reveals distinct differences in interpretation. The two equations take the same form if we make the substitutions

$$V \rightarrow A_z, \quad (\text{XX-116})$$

$$\rho \rightarrow J_z, \quad (\text{XX-117})$$

$$\epsilon_0 \rightarrow \frac{1}{\mu_0}, \quad (\text{XX-118})$$

$$\kappa_{eXX} \rightarrow \gamma_{YY}, \quad (\text{XX-119})$$

$$\kappa_{eXY} = \kappa_{eYX} \rightarrow -\gamma_{XY}, \quad (\text{XX-120})$$

$$\kappa_{eYY} \rightarrow \gamma_{XX}, \quad (\text{XX-121})$$

$$D_{cY} \rightarrow -H_{cX}, \quad (\text{XX-122})$$

$$D_{cX} \rightarrow H_{cY}. \quad (\text{XX-123})$$

The interchange of components and signs is equivalent to changing φ_E to $\varphi_E + 90$ degrees when the easy axis has a fixed direction. This is not simply an interchange of hard and easy axes.

H. Anisotropic magnetostatics in cylindrical coordinates

To find the correspondence between the cylindrical and Cartesian cases, one must return to Equation XX-99 and express the ∇ operator and cross products in cylindrical coordinates. By following the steps taken in deriving Equation XX-47 one finds that

$$\begin{aligned} & \oint_C \left[\frac{\gamma_{RR}}{r} \frac{\partial}{\partial Z} (-rA_\theta) - \frac{\gamma_{RZ}}{r} \frac{\partial}{\partial r} (-rA_\theta) + \mu_0 H_{cR} \right] dr \\ & + \oint_C \left[\frac{\gamma_{RZ}}{r} \frac{\partial}{\partial Z} (-rA_\theta) - \frac{\gamma_{ZZ}}{r} \frac{\partial}{\partial r} (-rA_\theta) + \mu_0 H_{cZ} \right] dz \\ & = \mu_0 \int_A (-J_\theta) dr dz. \end{aligned} \quad (\text{XX-124})$$

Comparison with Equation XX-103 gives the correspondences

$$rA_\theta \rightarrow -A_z, \quad (\text{XX-125})$$

$$J_\theta \rightarrow -J_z, \quad (\text{XX-126})$$

$$\frac{\gamma_{RR}}{r} \rightarrow \gamma_{XX}, \quad (\text{XX-127})$$

$$\frac{\gamma_{RZ}}{r} \rightarrow \gamma_{XY}, \quad (\text{XX-128})$$

$$\frac{\gamma_{ZZ}}{r} \rightarrow \gamma_{YY}, \quad (\text{XX-129})$$

$$H_{cR} \rightarrow H_{cX}, \quad (\text{XX-130})$$

$$H_{cZ} \rightarrow H_{cY}, \quad (\text{XX-131})$$

which are the analogue of Equations XX-50 through XX-52.

I. Anisotropic electrostatics in cylindrical coordinates

The starting point is Equation XX-113, which must be expressed cylindrical coordinates. The resulting equation is

$$\begin{aligned}
 & \oint_C \left[-\mathbf{r}\mathbf{\kappa}_{eZR} \frac{\partial V}{\partial r} - \mathbf{r}\mathbf{\kappa}_{eZZ} \frac{\partial V}{\partial z} + \frac{1}{\epsilon_0} (-r\mathbf{D}_{cZ}) \right] dr \\
 & + \oint_C \left[\mathbf{r}\mathbf{\kappa}_{eRR} \frac{\partial V}{\partial r} + \mathbf{r}\mathbf{\kappa}_{eRZ} \frac{\partial V}{\partial z} + \frac{1}{\epsilon_0} (r\mathbf{D}_{cR}) \right] dz \\
 & = \frac{1}{\epsilon_0} \int_A r \rho dr dz .
 \end{aligned} \tag{XX-132}$$

Comparison with Equation XX-103 gives the correspondences

$$V \rightarrow A_z, \tag{XX-133}$$

$$r\rho \rightarrow J_z, \tag{XX-134}$$

$$\epsilon_0 \rightarrow \frac{1}{\mu_0}, \tag{XX-135}$$

$$\mathbf{r}\mathbf{\kappa}_{eRR} \rightarrow -\gamma_{YY}, \tag{XX-136}$$

$$\mathbf{r}\mathbf{\kappa}_{eRZ} = \mathbf{r}\mathbf{\kappa}_{eZR} \rightarrow \gamma_{XY}, \tag{XX-137}$$

$$\mathbf{r}\mathbf{\kappa}_{eZZ} \rightarrow -\gamma_{XX}, \tag{XX-138}$$

$$r\mathbf{D}_{cR} \rightarrow \mathbf{H}_{cY}, \tag{XX-139}$$

$$r\mathbf{D}_{cZ} \rightarrow \mathbf{H}_{cX}. \tag{XX-140}$$